A preliminary study on the lithospheric thermal structure and rheology of the Tibetan plateau[*]

Yang Wang[✝]

Division of Petrology, School of Earth Sciences and Resources, China University of Geosciences, Beijing 100083, China

Abstract   The lithosphere temperature beneath the Tibetan plateau was estimated by local isostasy equilibrium constrained geothermal calculation. Maps of the lateral temperature variation at depths of 40 km, 70 km, and Moho are presented for the Tibetan plateau, and the thermal thickness of the lithosphere is also presented. The Tibetan plateau has a warm and thick lithospheres, but the thinner lithospheres are identified in the northern Tibet and the eastern margin of the plateau. The warm and soft lithospheres in the Tibetan plateau may represent a snapshot of the early stage of convective thinning of the convergent lithosphere. The "crème brûlée" layering demonstrates the rheological behavior of the Tibetan plateau.

Key words: geotherm; isostasy; rheology; lithosphere; Tibetan plateau
CLC number: P314.2   **Document code**: A

1 Introduction

The Tibetan plateau exhibits significant lateral variations of crustal structure, lithosphere thickness and temperature distributions (e.g. Wang, 2001; Klemperer, 2006; Zhang et al., 2011). Accordingly, the study on the thermal state and strength of the continental lithosphere in the Tibetan plateau provides not only insights on the present-day geodynamics for this geologically intriguing landmass, but also information about the spatial variability of lithospheric rheology in a highly heterogeneous region. Previous studies on the lithosphere thermal state of Tibetan plateau relied on the heat flow observations only (Huang et al., 1996a, b; Wang, 1996). Unfortunately, there lack sufficient observations in the most area of the Tibetan plateau (Wang and Huang, 1990; Wang, 1996; Hu et al., 2000, 2001; Wang, 2001). To avoid the difficulty from the biased geographic distribution and intrinsic errors of some heat flow observations, here we use local isostasy analysis to constrain the lithosphere temperature distributions of the Tibetan plateau. The $1° \times 1°$ grid based maps of the lateral temperature distributions at 40 km, 70 km, and Moho depths are presented, either maps of the thermal lithosphere thickness and the lithosphere strength. The results provide a more robust approximation to the lithosphere thermal structure and the rheology of the Tibetan plateau.

2 Geothermal modelling

2.1 Geothermal gradient reconstruction

Detailed descriptions on the methodology to reconstruct the lithospheric thermal structure can be found in Wang and Cheng (2012). An abbreviated outline is provided below.

Under 1-D steady state assumption the temperature distribution in the lithosphere is determined by the following equation:

$$-\mathrm{div}(-k\mathrm{grad}T) + A = 0, \qquad (1)$$

where k is the thermal conductivity ($\mathrm{W \cdot m^{-1} \cdot K^{-1}}$), T is temperature (°C), and A is radiogenic heat production ($\mathrm{\mu W \cdot m^{-3}}$).

Relative topographic variations, assuming local isostasy and taking into account density variations due

---

to thermal expansion in the lithospheric mantle, can be used to constrain the vertical distribution of temperature within the lithosphere (geotherm) (Zeyen and Fernandez, 1994). Assuming local isostatic conditions, the absolute elevation of a given lithospheric column is determined by comparing its buoyancy force with that of a reference column. Taking the reference column at the mid-oceanic ridges, the surface elevation is given by (Lachenbruch and Morgan, 1990)

$$E = \frac{\rho_a - \rho_l}{\rho_a}L - H_0 \quad E \geq 0, \qquad (2)$$

where E is elevation above sea level (m), ρ_a is density of the asthenosphere (kg·m^{-3}), ρ_l is mean density of the lithosphere (kg·m^{-3}), L is thickness of the lithosphere (m), and H_0 is depth below sea level of an unloaded asthenospheric mantle (m). In this study, H_0 is taken to be $-2\,400$ m, and the density of lithospheric mantle is assumed to increase upward with decreasing temperature (Lachenbruch and Morgan, 1990). Therefore

$$\rho_m(z) = \rho_a[1 + \alpha(T_a - T(z))], \qquad (3)$$

where $\rho_m(z)$ is density in the lithospheric mantle (kg·m^{-3}), α is thermal expansion coefficient (K^{-1}), T_a is temperature at the lithosphere-asthenosphere boundary

(LAB) (°C), and $T(z)$ is temperature in the lithospheric mantle (°C), and z is depth.

The mean elevation of each $1° \times 1°$ latitude-longitude grid derived from the ETOP5 model is used as the fitting target in this study. The trial-and-error method is applied to search the surface heat flow value and obtain a minimum misfit of the elevation in each $1° \times 1°$ grid. The misfit (m) is expressed as

$$m = \frac{E_0 - E_c}{E_0 - H_0} \times 100\%, \qquad (4)$$

where E_0 is the mean elevation above sea level of each grid from the ETOP5 model, and E_c is the calculated elevation above sea level for each grid, and H_0 is depth below sea level of an unloaded asthenospheric mantle ($-2\,400$ m).

The geotherm calculation procedure adopts a five-layer model, consisting of a sedimentary layer (where present), an upper crust, an upper lower crust, and the lowermost crust, as well as, the lithospheric mantle layer. The heat production is assumed as stepwise distributions with depth (Wang, 2005a, b; Wang and Du, 2004 a, b; Wang and Deng, 2001; Xia et al., 2006; Wang and Sun, 2010). All thermophysical parameters adopted for the geotherm calculation are summarized in Table 1.

Table 1 Parameters used in the local isostasy constrained geotherm modelling

Radiogenic heat production for sedimentary layer, $A_s/(\mu W \cdot m^{-3})$	1.3
Radiogenic heat production for upper crust, $A_{uc}/(\mu W \cdot m^{-3})$	1.3
Radiogenic heat production for upper lower crust, $A_{lc}/(\mu W \cdot m^{-3})$	0.4
Radiogenic heat production for lowermost crust, $A_{lc2}/(\mu W \cdot m^{-3})$	0.2
Radiogenic heat production for mantle, $A_m/(\mu W \cdot m^{-3})$	0.002
Thermal conductivity of sedimentary layer, $k_s/(W \cdot m^{-1} \cdot K^{-1})$	2.5
Thermal conductivity of upper crust, $k_{uc}/(W \cdot m^{-1} \cdot K^{-1})^{(1)}$	$k_0(1+cz)/(1+b\Delta T)$, k_0=3.0
Thermal conductivity of upper lower crust, $k_{lc}/(W \cdot m^{-1} \cdot K^{-1})^{(2)}$	$k_0(1+cz)/(1+b\Delta T)$, k_0=2.6
Thermal conductivity of lowermost crust, $k_{lc2}/(W \cdot m^{-1} \cdot K^{-1})^{(2)}$	$k_0(1+cz)/(1+b\Delta T)$, k_0=2.6
Thermal conductivity of mantle, $k_m/(W \cdot m^{-1} \cdot K^{-1})^{(3)}$	$0.368 \times 10^{-9}\, T^{-3} + 1/(0.174 + 0.000265T)$
Density of seawater, $\rho_w/(kg \cdot m^{-3})$	1 030
Density of sedimentary layer, $\rho_s/(kg \cdot m^{-3})^{(4)}$	2 400
Density of upper crust, $\rho_{uc}/(kg \cdot m^{-3})^{(4)}$	2 750
Density of upper lower crust, $\rho_{lc}/(kg \cdot m^{-3})^{(4)}$	2 900
Density of lowermost crust, $\rho_{lc2}/(kg \cdot m^{-3})^{(4)}$	2 970
Density of lithospheric mantle, $\rho_m/(kg \cdot m^{-3})^{(5)}$	$\rho_a[1+\alpha(T_a-T(z))]$
Density of asthenospheric mantle, $\rho_a/(kg \cdot m^{-3})^{(6)}$	3 200
Thermal expansion coefficient, $\alpha/K^{-1(6)}$	3.5×10^{-5}
Depth below sea level of an unloaded asthenospheric mantle, H_0/m	$-2\,400$
Acceleration of gravity, $g/(m \cdot s^{-2})$	9.81
Universal gas constant, $R/(J \cdot mol^{-1} \cdot K^{-1})$	8.314
Steady-state strain rate, $\dot{\varepsilon}/s^{-1}$	10^{-15}

Note: [1] b=1.5×10^{-3} K^{-1}, c=1.5×10^{-3} km^{-1} (Chapman and Furlong, 1992). [2] b=1.0×10^{-4} K^{-1}, c=1.5×10^{-3} km^{-1} (Chapman and Furlong, 1992). [3] The unit of T is degree Kelvin (Doin and Fleitout, 1996). [4] According to the experimentally determined v_P-density relationship (Christensen and Mooney, 1995). [5] T_a represents the temperature at the lithosphere-asthenosphere boundary, 1 350 °C. [6] The values follow Lachenbruch and Morgan (1990).

The thickness of crust and its sub-layers are obtained from a 1°×1° grid crustal v_P model of the Tibetan plateau and its adjacent region (Zhu et al., 2002, 2004; Li et al., 2004; Gao et al., 2005), which covers a rectangular region from 20°N–42°N and 73°E–108°E. For each grid, the uppermost layer with v_P less than 5.4 km·s^{-1} are taken as sedimentary layers; and the layer with v_P of 5.4 to 6.4 km·s^{-1} is defined as upper crust. In the lower part of crust, the layer with v_P in range from 6.4 to 6.8 km·s^{-1} is adopted as the upper lower crust; and the remaining portion with v_P higher than 6.8 km·s^{-1} is taken as the lowermost crust. The densities of sedimentary layer, upper crust, upper lower crust, lowermost crust, and mantle are listed in Table 1.

2.2 Sensitivity analysis

For the local isostasy-based procedure used in this study, the main uncertainty for modelling result comes from the estimation of the mean crustal density, which is much less than that of the mantle and is determined by the composition and thickness of sub-layers of the crust. Because the v_P-density relationship established by experiments is robust (Christensen and Mooney, 1995; Rudnick and Fountain, 1995), the estimate for layer thickness is more critical for our sensitivity analysis. We select five grids representing various tectonic settings as reference models for sensitivity analysis. In calculation, the thickness increases/decreases 1 km for each sub-layers of crystalline crust (excluding sedimentary layer), with a total variation of 3 km for the whole crust, to determine the sensitivity of our procedure. The results are presented in Table 2.

The sensitivity analysis shows that the Moho temperature is relative insensitive to the 3 km variation of the crustal thickness, either are the temperatures at 40 km and 70 km depths. The maximum variation of temperature at 40 km depth is less than 25 °C. Meanwhile the maximum variation of temperature at 70 km depth is less than 50 °C, and is consistent with the accuracy of the downward continuation calculation for geothermal modelling (Jokinen and Kukkonen, 1999; Artemieva and Mooney, 2001). However, the lithosphere thickness is relatively sensitive to the crustal variation, because of the significant density contrast between crust and mantle. In most cases, a 3 km variation of crustal thickness causes a 9%–16% depth change of the LAB.

Table 2 Sensitivity analysis for local isostasy constrained geotherm modelling

Location	Lat. /°N	Long. /°E	Moho /km	$\Delta T_{\text{Moho}}^{\text{a}}$/°C		$\Delta T_{40\ \text{km}}^{\text{b}}$/°C		$\Delta T_{70\ \text{km}}^{\text{c}}$/°C		ΔL^{d}	
				+3$^{\text{e}}$ km	−3$^{\text{f}}$ km	+3$^{\text{e}}$ km	−3$^{\text{f}}$ km	+3$^{\text{e}}$ km	−3$^{\text{f}}$ km	+3$^{\text{e}}$ km	−3$^{\text{f}}$ km
Qilianshan	38.5	98.5	64	+5	+28	+5	+23	−9	+49	+15%	−19%
Qaidam	37.5	94.5	54	+21	−10	+13	−2	+2	+16	+10%	−11%
N. Tibet	33.5	85.5	71	−37	+31	−22	+22	−48	+48	+23%	−14%
E. Tibet	33.5	98.5	71	+20	+17	+19	+9	+12	+29	+9%	−16%
S. Tibet	29.5	90.5	72	−19	+15	−15	+8	−27	+27	+25%	−15%

Note: $^{\text{a}}$ Variation of temperature at Moho. $^{\text{b}}$ Variation of temperature at 40 km depth. $^{\text{c}}$ Variation of temperature at 70 km depth. $^{\text{d}}$ Relative variation of lithosphere thickness. $^{\text{e}}$ Crustal thickness 3 km more than reference value in the grid. $^{\text{f}}$ Crustal thickness 3 km less than reference value in the grid.

It is suggested that the uncertainty of geothermal modelling due to the crustal structure variation in the Tibetan plateau is not significant. Deep seismic sounding profiles, the basis of the crust model used in this study, had covered the major tectonic domains of the Tibetan plateau (Xiong and Liu, 1997; Zhao et al., 2001; Galvé et al., 2002; Wang et al., 2003; Li et al., 2004; Zhang et al., 2011 and references herein). Accordingly, the accuracy of the crustal v_P model of the western Chinese mainland is warranted, with error of crustal thickness in each 1°×1° grid less than 2 km. Therefore, the uncertainty of geothermal modelling for the Tibetan plateau presented here is acceptable for regional scale studies.

3 Calculation of lithosphere rheology

Laboratory rock mechanics studies demonstrate a dependence of rock-strength on temperature and pressure (e.g., Goetze and Evans, 1979). Within the mechanically strong part of the lithosphere, the strength of the upper part is defined by criteria for brittle failure (Byerlee's Law). Creep processes become dominant at temperatures exceeding roughly half the melting temperature of rock (Carter and Tsenn, 1987). Therefore, the strength in the lower part of the lithosphere and the lower part of crust is governed by the temperature

distribution. Extrapolation of flow laws and laboratory failure criteria (i.e., Byerlee, 1978; Brace and Kohlstedt, 1980) and adopting estimates for tectonic strain-rates and thermal gradients at different depths provide a first-order description of the strength distribution within the lithosphere. For each depth interval, strengths for both brittle and ductile deformation were calculated, with the lesser of these representing the limiting strength of the lithosphere (σ_v) at that particular depth level (e.g., Ranalli, 1995).

The Byerlee's Law can be expressed as (Sibson, 1974)

$$\sigma_{\mathrm{brittle}} = \sigma_1 - \sigma_3 = \alpha\rho\mathrm{g}z(1 - \lambda), \qquad (9)$$

where α is a parameter depending on the type of faulting, ρ the average density, g the gravity acceleration, z is the depth and λ is the pore fluid factor. In this study, we take α=3.0 (thrust faulting) and a typical ("hydrostatic") λ=0.37.

Power-creep law is expressed as (Ranalli, 1995)

$$\sigma_{\mathrm{creep}} = \sigma_1 - \sigma_3 = (\frac{\dot{\varepsilon}}{A})^{\frac{1}{n}} \exp(\frac{Q}{nRT}), \qquad (10)$$

where $\dot{\varepsilon}$ is the steady-state strain rate, T the temperature in degree Kelvin, R the universal gas constant, A

and n are material creep parameters, and Q the activation energy.

A scalar measure for the total strength of a multi-layer lithosphere with a depth-dependent rheology can be obtained by vertically integrating the yield envelope:

$$S_{\mathrm{L}} = \int_0^h \sigma_v \mathrm{d}z, \qquad (11)$$

where S_{L} is the integrated lithospheric strength.

In calculation, a four-layer model, consisting of an upper crust (wet quartzite), the upper lower crust (felsic granulite), a lowermost crust (mafic granulite), and the upper mantle (wet peridotite) is adopted; meanwhile, a steady-state strain rate $\dot{\varepsilon}$ of 10^{-15} s^{-1} is used. Parameters used for rheological modelling are presented in Tables 1 and 3.

Following Afonso and Ranalli (2004), we calculated relative crust strength for the Tibetan plateau, as the percentage of the crust strength to the integrated strength of whole lithosphere, because the "crème brûlée" here is regarded as all models with a weak mantle but "jelly sandwich" as all models with a strong mantle, not just those with a weak lower crust (Burov and Watts, 2006).

Table 3　Creep parameters for lithospheric rocks

Lithology	Powerlaw exponent n	Powerlaw activation energy Q/(kJ·mol^{-1})	Pre-exponential constant (powerlaw) A/(MPa^{-n}·s^{-1})	Source
Wet quartzite	2.3	154	2.0×10^{-4}	Kirby and Kronenberg (1987)
Felsic granulite	3.1	243	8.0×10^{-3}	Wilks and Carter (1990)
Mafic granulite	4.2	445	1.4×10^4	Wilks and Carter (1990)
Wet peridotite	4.0	471	2.0×10^3	Chopra and Paterson (1984) Chopra and Paterson (1981)

4 Results and discussion

The estimated values of surface heat flow are shown in Figure 1. There exists good agreement between the inverted and the observed heat flow values in the Tibetan plateau and its adjacent regions. The inverted heat flow values for the main portion of the Tibetan plateau are in the range of 65–72 mW·m^{-2}. Hu et al. (2000) argued that the seven unpublished heat flow values from oil company drillings in western Tibet are quite similar to those in eastern Tibet. According to these authors, the measured values are in the range of 61–77 mW·m^{-2} for eastern Tibet, when some extreme values from southern Tibet are excluded. The inversion also displays good agreements for the Qilian-shan belt (60−65 mW·m^{-2}) and the Qaidam basin (60–

65 mW·m^{-2}) (Wang, 1996; Wang et al., 1996; Wang, 2001). Hence, we suggest our inverted heat flow values may approximate the conductive heat flux from the deep Tibetan plateau.

The lithosphere temperatures for the Tibetan plateau and its surrounding regions are displayed in map view for the depths of 40 km, 70 km, and the depth of the Moho (Figures 2–4). At the same depth, the highest temperatures are present within the Tibetan plateau, and the temperatures under the Tarim and the Sichuan basin are much lower. The temperature difference between the tectonically active Tibetan plateau and its surrounding stable regions is greater than 200 °C. For example, the temperatures at 40 km depth are higher than 800 °C under the major portion of the Tibetan plateau, but lower than 600 °C under the
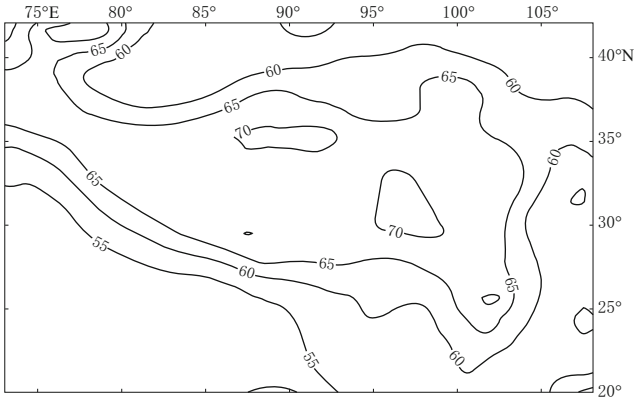
Figure 1   Inverted surface heat flow values for the Tibetan plateau and its adjacent areas (1°×1° Kriging interpolation).
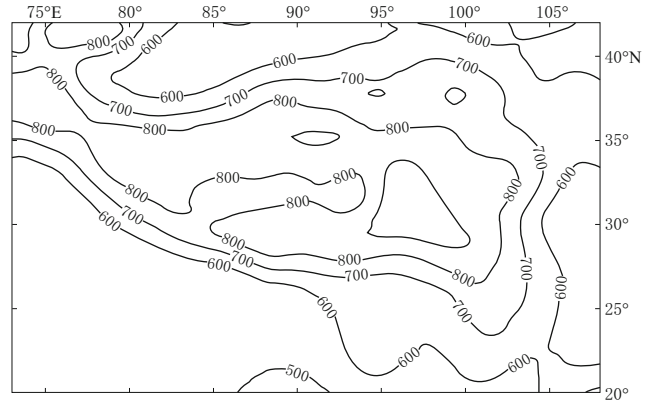

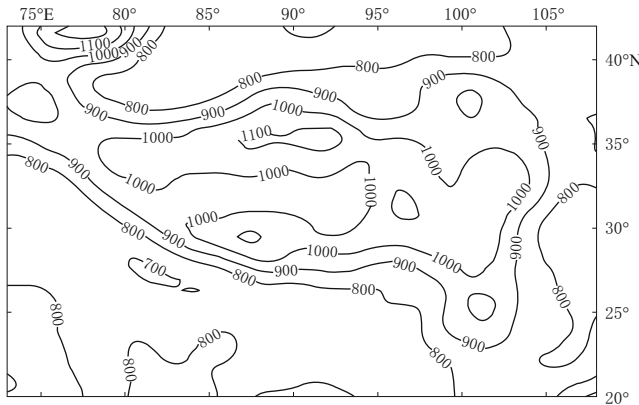**Figure 2**   Estimated temperatures at 40 km depth (1°×1° Kriging interpolation).

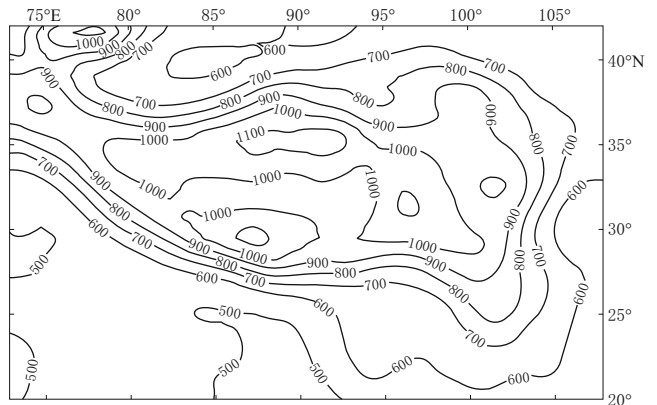**Figure 3**   Estimated temperatures at 70 km depth (1°×1° Kriging interpolation).

Figure 4   Estimated temperatures at the depth of the Moho (1°×1° Kriging interpolation).

Tarim basin (Figure 2). At the depth of the Moho, the typical temperatures are estimated to be 550–650 °C in the Tarim basin (where the crust is 45 to 50 km thick); and more than 700 °C in the thick-crust regions (where the Moho is >50 km); such as the Qaidam basin and the Qilianshan fold belt, as well as the interior of Tibetan plateau. The highest value of Moho temperature within the Tibetan plateau reaches 1 200 °C (Figure 4). There exists good agreement between the Moho temperatures and the P-wave velocities of the uppermost mantle (P_n). The P_n tomography (Hearn et al., 2004; Liang et al., 2004; Pei et al., 2007) shows that the low values occur beneath the northern Tibet and the eastern margin of the plateau, but the high values occur beneath the Tarim and Sichuan basins.

Many geophysical evidences such as the crustal high conductivity zones from natural-source magnetotelluric (MT), the plateau-wide low crustal velocity from seismic studies, as well as the shallow depth (*ca.* 15 km) of Curie isotherm across the entire plateau, suggest the existence of a hot crust in the Tibetan plateau (cf. Klemperer, 2006). Lebedev and Agius (2009) also identified widespread mid-crust low velocity layer in the Tibetan plateau from surface wave inversion. Meanwhile, the Miocene potassic volcanic rocks in southern Tibet (Ding et al., 2003), as well as the Late Miocene to recent potassic volcanic rocks in the northern Tibet represent the high temperature (*ca.* 1 100°C) melting of the subcontinental mantle (Turner et al., 1996). Accordingly, our thermal study confirms that the entire lithosphere of the Tibetan plateau is hot as suggested by a significant number of geophysical and geological observations (Klemperer, 2006; McKenzie and Priestley, 2008).

The thickness of the thermal lithosphere, here defined as a conductive layer above the 1 350 °C isotherm, is more than 120 km in the Tibetan plateau (Figure 5).
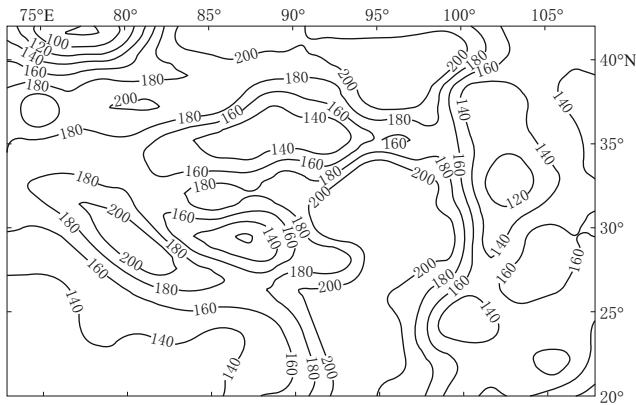
Figure 5 Lithospheric thermal thickness beneath the Tibetan plateau and its adjacent areas ($1° \times 1°$ Kriging interpolation), assumed to be the depth of the 1 350 °C isotherm.

The lithospheric bulge in the eastern Tibet has thickness of 200−240 km. The lithosphere beneath the Qilianshan fold belt is 200 km thick or more. The thicker lithosphere (160–180 km) also occurs beneath the Tarim and the Sichuan basins. However, the thinner lithosphere (<140 km) occurs beneath northern Tibet and the eastern margin of the Tibetan plateau (east of 100°E median).

The lithospheric thermal thickness of the Tibetan plateau attained by this study is consistent with that from seismic studies. The upper mantle structure implied by P_n travel-time tomography (McNamara et al., 1997) and by S-wave velocity anomalies determined from the inversion of fundamental mode Love and Rayleigh waves (Villaseñor et al., 2001) suggests that extreme thinning of the lithospheric mantle occurs beneath northern Tibet. Surface wave inversion by Agius and Lebedev (2009) confirms that a thicker (160–180 km) lithosphere exists beneath southern Tibet, but thinner lithospheric mantle under the northern Tibet. From the vertical distribution of shear wave velocity, McKenzie and Priestley (2008) argued that the lithosphere beneath the main portion of the Tibetan plateau is thicker than 180 km. Meanwhile, recent seismic tomography studies suggest that there exists a much thinner lithosphere (<140 km) beneath the eastern margin of the Tibetan plateau (Feng et al., 2011; Hu et al., 2011). The agreement between thermal modelling and seismic studies means that the geotherms constructed by isostatic equilibrium constraint are reliable.

The thick but warm lithospheres under the Tibetan plateau, and the Qilianshan fold belt correspond to the shortening caused by the convergence of the Indian and the Eurasian plates (Revenaugh and Sipkin, 1994). Houseman and Molnar (2001) pointed out that the thickened lithospheric mantle can cause a disturbance to the rheologically stratified system, which induces Rayleigh-Taylor instability with the denser layer descending as a viscous drop and finally results in the convective thinning of the lithospheric mantle in convergent environments. According to seismic evidence, Houseman and Molnar (2001) suggested that the lithospheric mantle beneath the Tibetan plateau had undergone some form of instability that has led to asthenospheric replacement of some part of the lithospheric mantle. Meanwhile, the basaltic volcanism erupted since *ca*. 10 Ma, especially in the northern Tibet, also implies a thinner lithosphere in the northern Tibet (Arnaud et al., 1992; Turner et al., 1996). Therefore, the results of our geothermal modelling confirm the argument that the current structure of the lithosphere beneath the Tibetan plateau is a snapshot of the early stages of lithosphere instability (Revenaugh and Sipkin, 1994).

The lateral distribution of the integrated lithospheric strength in the Tibetan plateau and its surrounding area is presented in Figure 6, and the relative strength ratios are shown in Figure 7. It is shown that the lithospheric strength is lower than 2×10^{12} Pa·m within the Tibetan plateau, due to its over-thickened crust and elevated geotherm. The percentage of the crust strength to the integrated strength of the entire lithosphere across the majority of Tibetan plateau is larger than 90% (Figure 7), corresponding to a stronger crust, but a weak upper mantle. This means that the present-day rheology of the Tibetan plateau belongs to the typical "crème-brûlée" layering. Previous studies point to the weak (<1×10^{13} Pa·m) strength of the "crème-brûlée" layering as being earthquake-prone (Wang, 2001; Wang and Cheng, 2012). Accordingly, the high intensity of seismic activity in the Tibetan plateau is determined by rheological characteristics of the lithosphere. Meanwhile, the existence of weak lower crust and upper mantle beneath the Tibetan plateau favors the "channel flow" model of the large-scale deformation (Klemperer, 2006; Beaumont et al., 2006).
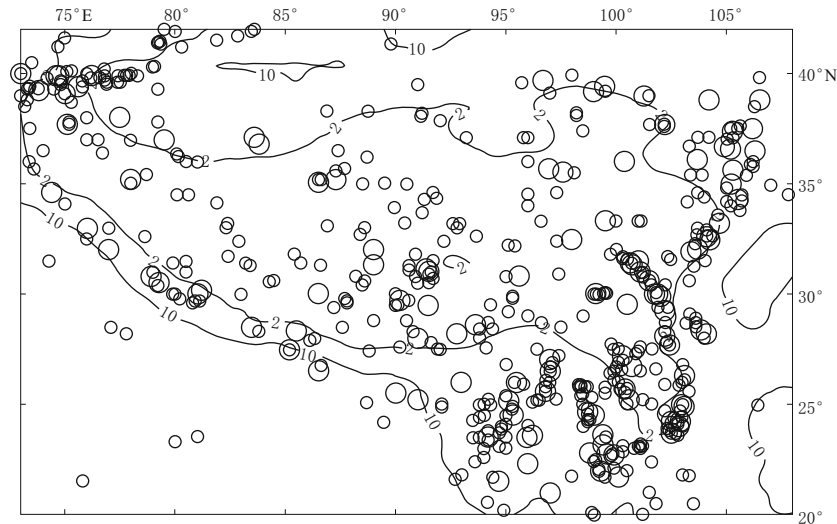
Figure 6   Integrated lithospheric strength (in the unit of 10^{12} Pa·m) of the Tibetan plateau and adjacent areas presented with $1° \times 1°$ Kriging interpolation. Large circle represents the epicenter of $M_S \geq 7.0$ earthquake, and small circle represents the epicenter of $6.0 \leq M_S < 7.0$ earthquake (earthquake catalogue is from Song et al., 2011).

Figure 7   Distribution of the percentage of crust strength relative to lithospheric strength in the Tibetan plateau and adjacent areas presented with $1° \times 1°$ Kriging interpolation. Large circle represents the epicenter of $M_S \geq 7.0$ earthquake, and small circle represents the epicenter of $6.0 \leq M_S < 7.0$ earthquake (earthquake catalogue is from Song et al., 2011).
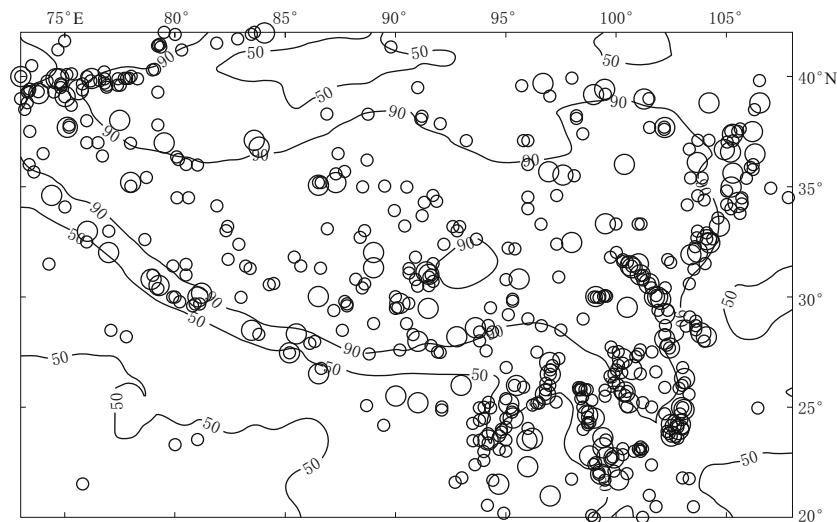
5 Conclusions

The geothermal modelling constrained by local isostatic equilibrium offers reliable estimates for the temperature variations within the lithosphere beneath the Tibetan plateau. In general, the Tibetan plateau is characterized by a warm and thick lithosphere. The temperatures at 40 km depth are higher than 800 °C under the major portion of the Tibetan plateau. The typical temperatures at Moho depth are more than 700 °C in the interior of Tibetan plateau, and the highest value reaches 1 200 °C. The thickness of the thermal lithosphere is more than 200 km beneath eastern Tibet and the Qilianshan fold belt. Meanwhile, the lithosphere is less than 140 km beneath northern Tibet and the eastern margin of the Tibetan plateau. The thick and hot lithosphere under the Tibetan plateau results from the uniform thickening of the crust and lithospheric mantle.

However, the thin thermal lithosphere under the northern Tibet indicates the onset of convective thinning. The conclusions of geothermal modeling, presented in this study, are consistent with the results from seismic tomography. The lithospheric rheology of the Tibetan plateau is approximated by the "crème brûlée" layering model, characterized by a strong crust with a weak upper mantle.

References

Afonso J C and Ranalli G (2004). Crustal and mantle strengths in continental lithosphere: Is the jelly sandwich model obsolete? *Tectonophysics* **394**: 221–232.

Agius M and Lebedev S (2009). Surface-wave phase-velocity analysis across the Tibetan plateau using broadband inter-station dispersion measurements. Abstracts of 5th International Symposium on the Tibetan plateau and 24th Himalaya-Karakorum-Tibet Workshop, 11–14 August 2009, Beijing, China, 258.

Arnaud N O, Vidal Ph, Tapponnier P, Matte Ph and Deng W M (1992). The high K_2O volcanism of northwestern Tibet: Geochemistry and tectonic implications. *Earth Planet Sci Lett* **111**: 351–367.

Artemieva I M and Mooney W D (2001). Thermal thickness and evolution of Precambrian lithosphere: A global study. *J Geophys Res* **106**: 16 387–16 414.

Beaumont C, Nguyen M H, Jamieson R A and Ellis S (2006). Crustal flow modes in large hot orogen. In: Law R D, Searle M P and Godin L eds. *Channel Flow, Ductile Extrusion and Exhumation in Continental Collision Zones*. Special Publications. Geological Society, London, **268**: 91–145.

Brace W F and Kohlstedt D L (1980). Limits on lithospheric stress imposed by laboratory experiments. *J Geophys Res* **85**: 6 248–6 252.

Burov E B and Watts A B (2006). The long–term strength of continental lithosphere: "jelly sandwich" or "crème brûlée"? *GSA Today* **16**: 4–10.

Byerlee J (1978). Friction of rocks. *Pure Appl Geophys* **116**: 615–626.

Carter N L and Tsenn M C (1987). Flow properties of continental lithosphere. *Tectonophysics* **136**: 27–63.

Chapman D S and Furlong K P (1992). Thermal state of the continental lower crust. In: Fountain D M, Arculus R and Kay R W eds. *Continental Lower Crust*. Elsevier, Amsterdam, 179–199.

Chopra P N and Paterson M S (1981). The experimental

deformation of dunite. *Tectonophysics* **78**: 453–473.

Chopra P N and Paterson M S (1984). The role of water in the deformation of dunite. *J Geophys Res* **89**: 7 861–7 876.

Christensen N I and Mooney W D (1995). Seismic velocity structure and composition of the continental crust: A global view. *J Geophys Res* **100**: 9 761–9 788.

Ding L, Kapp P, Zhong D and Deng W (2003). Cenozoic volcanism in Tibet: Evidence for a transition from oceanic to continental subduction. *J Petrol* **44**: 1 833–1 865.

Doin M P and Fleitout L (1996). Thermal evolution of the oceanic lithosphere: An alternative view. *Earth Planet Sci Lett* **142**: 121–136.

Feng M, An M, Zhao W, Xue G, Mechie J and Zhao J (2011). Lithosphere structures of northeast Tibetan plateau and their geodynamic implications. *Journal of Geodynamics* **52**: 432–442.

Galvé A, Hirn A, Jiang M, Gallart J, Voogd B, Lépine J C, Diaz J, Wang Y X and Qian H (2002). Modes of raising northeastern Tibet probed by explosion seismology. *Earth Planet Sci Lett* **203**: 35–43.

Gao X, Wang W M and Yao Z X (2005). Crustal structure of China mainland and its adjacent regions. *Chinese J Geophys* **48**: 591–601 (in Chinese with English abstract).

Goetze C and Evans B (1979). Stress and temperature in the bending lithosphere as constrained by experimental rock mechanics. *Geophys J R astr Soc* **59**: 463–478.

Hearn T M, Wang S, Ni J F, Xu Z, Yu Y and Zhang X (2004). Uppermost mantle velocities beneath China and surrounding regions. *J Geophys Res* **109**: B11301, doi:10.1029/2003JB002874.

Houseman G and Molnar P (2001). Mechanisms of lithospheric rejuvenation associated with continental orogeny. In: Miller J A, Holdsworth R E, Buick I S and Hand M eds. *Continental Reactivation and Reworking*. Special Publications. Geological Society, London, **184**: 13–38.

Hu J, Xu X, Yang H, Wen L and Li G (2011). S receiver function analysis of the crustal and lithospheric structures beneath eastern Tibet. *Earth Planet Sci Lett* **306**: 77–85.

Hu S, He L and Wang J (2000). Heat flow in the continental area of China: A new data set. *Earth Planet Sci Lett* **179**: 407–419.

Hu S, He L and Wang J (2001). Compilation of heat flow data in the China continental area (3rd edition). *Chinese J Geophys* **44**: 611–626 (in Chinese with English abstract).

Huang S, Wang J Y and Chen M (1996a). The map of temperature at Moho (1:12 000 000). In: Yuan X C ed. *Atlas of Geophysics in China*. Publication No. 201 of the International Lithosphere Program. Geological Publishing House, Beijing, 106–107.

Huang S, Wang J Y and Chen M (1996b). The map of thickness of the thermal lithosphere (1:12 000 000). In: Yuan

X C ed. *Atlas of Geophysics in China*. Publication No. 201 of the International Lithosphere Program. Geological Publishing House, Beijing, 108–109.

Jokinen J and Kukkonen I T (1999). Random modelling of the lithospheric thermal regime: Forward simulations applied in uncertainty analysis. *Tectonophysics* **306**: 277–292.

Kirby S H and Kronenberg A K (1987). Rheology of the lithosphere: Selected topics. *Rev Geophys* **25**: 1 219–1 244.

Klemperer S L (2006). Crustal flow in Tibet: Geophysical evidence for the physical state of Tibetan lithosphere, and inferred patterns of active flow. In: Law R D, Searle M P and Godin L eds. *Channel Flow, Ductile Extrusion and Exhumation in Continental Collision Zones*. Special Publications. Geological Society, London, **268**: 39–70.

Lachenbruch A H and Morgan P (1990). Continental extension, magmatism and elevation: Formal relations and rules of thumb. *Tectonophysics* **174**: 39–62.

Lebedev S and Agius M (2009). Seismic structure of Tibet: New constraints from surface waves. Abstracts of 5th International Symposium on the Tibetan plateau and 24th Himalaya-Karakorum-Tibet Workshop, 11–14 August 2009, Beijing, China, 30.

Li Q S, Peng S P and Gao R (2004). A review on the Moho discontinuity beneath the Tibetan plateau. *Geological Review* **50**: 598–612 (in Chinese with English abstract).

Liang C, Song X and Huang J (2004). Tomographic inversion of Pn travel times in China. *J Geophys Res* **109**: B11304, doi:10.1029/2003JB002789.

McKenzie D and Priestley K (2008). The influence of lithospheric thickness variations on continental evolution. *Lithos* **102**: 1–11.

McNamara D E, Walter W R, Owens T J and Ammon C J (1997). Upper mantle velocity structure beneath the Tibetan plateau from Pn travel-time tomography. *J Geophys Res* **102**: 493–505.

Pei S, Zhao J, Sun Y, Xu Z, Wang S, Liu H, Rowe C A, Toksöz M N and Gao X (2007). Upper mantle seismic velocities and anisotropy in China determined through Pn and Sn tomography. *J Geophys Res* **112**: B05312, doi:10.1029/2006JB004409.

Ranalli G (1995). *Rheology of the Earth* (2*nd Edition*). Chapman and Hall, London, 413pp.

Revenaugh J and Sipkin S A (1994). Mantle discontinuity structure beneath China. *J Geophys Res* **99**: 21 911–21 927.

Rudnick R L and Fountain D M (1995). Nature and composition of the continental crust: a lower crustal perspective. *Rev Geophys* **33**: 267–309.

Sibson R H (1974). Frictional constraints on thrust, wrench and normal faults. *Nature* **249**: 542–544.

Song Z P, Zhang G M and Liu J (2011). *Global Earthquake Catalog* (9999 *B.C. to A.D.* 1963 *M*≥5.0; *A.D.* 1964 *to*

A.D. 2010 *M*≥6.0). Seismological Press, Beijing, 450pp.

Turner S P, Arnaud N, Liu J, Rogers N, Hawkesworth C, Harris N, Kelley S P, van Calsteren P and Deng W (1996). Post-collison, shoshonitic volcanism on the Tibetan plateau: Implications for convective thinning of the lithosphere and the source of ocean island basalt. *J Petrol* **37**: 45–71.

Villaseñor A, Ritzwoller M H, Levshin A L, Barmin M P, Spakman W, Trampert J and Engdahl E R (2001). Shear velocity structure of central Eurasia from inversion of surface wave velocities. *Phys Earth Planet Inter* **123**: 169–184.

Wang C Y, Han W B, Wu J P, Lou H and Bai Z M (2003). Crustal structure beneath the Songpan-Garze orogenic belt. *Acta Seismologica Sinica* **16**: 229–241.

Wang J Y ed. (1996). *Geothermics in China*. Seismological Press, Beijing, 1–299.

Wang J Y and Huang S (1990). Compilation of heat flow data the China continental area (2nd edition). *Seismology and Geology* **12:** 359–366.

Wang J Y, Huang S and Chen M (1996). The map of terrestrial heat flow (1:12 000 000). In: Yuan X C ed. *Atlas of Geophysics in China*. Publication No. 201 of the International Lithosphere Program. Geological Publishing House, Beijing, 102–103.

Wang Y (2001). Heat flow pattern and lateral variations of lithosphere strength in China mainland: Constraints on active deformation. *Phys Earth Planet Inter* **126**: 121–146.

Wang Y (2005a). Comparison of element abundances between the exposed crust of the continent of China and the global average continental upper crust: constraints on the crustal evolution and some speculations. *Geological Bulletin of China* **24**: 906–915 (in Chinese with English abstract).

Wang Y (2005b). Element geochemical characteristics of the supra-crust of eastern Junggar region, Xinjiang and its geological implication. *Beijing Geology* **17**(2): 14–19 (in Chinese with English abstract).

Wang Y and Cheng S H (2012). Lithospheric thermal structure and rheology of the eastern China. *Journal of Asian Earth Sciences* **47**: 51–63.

Wang Y and Deng J (2001). Lateral variation of crustal composition in China as revealed by heat flow study. *Earth Science — Journal of China University of Geosciences* **26**: 597–602 (in Chinese with English abstract).

Wang Y and Du P (2004a). Element geochemical characteristics of the supra-crust of Tianshan Region. *Bulletin of Mineralogy, Petrology and Geochemistry* **23**: 5–9 (in Chinese with English abstract).

Wang Y and Du P (2004b). Element geochemical characteristics of the supra-crust of Altay range in China. *Global Geology* **23**: 144–148 (in Chinese with English abstract).

Wang Y and Sun Z M (2010). Crustal composition of China

continent constrained from heat flow data and helium isotope ratio of underground fluid. *Acta Geologica Sinica* (*English Edition*) **84**: 178–184.

Wilks K R and Carter N L (1990). Rheology of some continental lower crustal rocks. *Tectonophysics* **182**: 57–77.

Xia X F, Wang Y and Du P (2006). Geological significance of the element geochemical characteristics of the supracrust of Western Junggar region, Xinjiang. *Xinjiang Geology* **20**: 21–25 (in Chinese with English abstract).

Xiong S B and Liu H B (1997). Crustal structure in western Tibet Plateau. *Chinese Science Bulletin* **42**: 665–668 (in Chinese with English abstract).

Zeyen H and Fernandez M (1994). Integrated lithospheric modeling combing thermal, gravity, and local isostasy analysis: Application to the NE Spanish geotransect. *J Geophys Res* **99**: 18 089–18 102.

Zhang Z J, Yang L Q, Teng J W and Badal J (2011). An overview of the earth crust under China. *Earth Science Reviews* **104**: 143–166.

Zhao W, Mechie J, Brown L D, Guo J, Haines S, Hearn T, Klemperer S L, Ma Y S, Meissner R, Nelson K D, Ni J F, Pananont P, Rapine R, Ross A and Saul J (2001). Crustal structure of central Tibet as derived from project INDEPTH wide-angle seismic data. *Geophys J Int* **145**: 486–498.

Zhu J S, Cao J M. and Cai X L (2002). High resolution surface wave tomography in east Asia and west Pacific marginal seas. *Chinese J Geophys* **45**: 679–698 (in Chinese with English abstract).

Zhu J S, Cao J M, Cai X L and Yan Z Q (2004). The structure of lithosphere in Eurasia and West Pacific. *Advance in Earth Sciences* **19**: 387–392 (in Chinese with English abstract).